# A Cavitation Susceptibility Meter With Optical Cavitation Monitoring—Part Two: Experimental Apparatus and Results

**L. d'Agostino**[1]

**A. J. Acosta**

California Institute of Technology, Pasadena, CA 91125

*This work is concerned with the development and operation of a Cavitation Susceptibility Meter based on the use of a venturi tube for the measurement of the active cavitation nuclei concentration in water samples as a function of the applied tension. The pressure at the venturi throat is determined from the upstream pressure and the local flow velocity without corrections for viscous effects because the flow possesses a laminar potential core in all operational conditions. The detection of cavitation and the measurement of the flow velocity are carried out optically by means of a Laser Doppler Velocimeter. A custom-made electronic Signal Processor is used for real time data generation and temporary storage and a computerized system for final data acquisition and reduction. The implementation of the whole system is described and the results of the application of the Cavitation Susceptibility Meter to the measurement of the water quality of tap water samples are presented and critically discussed with reference to the current state of knowledge on cavitation inception.*

## 1 Introduction

Experience shows (Knapp et al., 1970) that the maximum tensile stress that liquids can theoretically sustain according to thermodynamic considerations is much larger than observed in practice. It has therefore been postulated that the tensile strength of liquids is considerably reduced by the presence of weak spots, generically called "nuclei," which act as preferential points for the onset of liquid rupture. The concentration and susceptibility of nuclei profoundly affect the inception, development, and scaling of cavitation in a wide variety of technically important applications. Therefore significant efforts have been made to develop effective cavitation nuclei detection methods (Billet, 1986; Billet, 1985; Oldenziel et al., 1982; Godefroy et al., 1981). Commonly used techniques, like Coulter counters, acoustical attenuation, acoustical and optical scattering, photography and holography, monitor noncavitating liquids and therefore cannot provide reliable information on cavitation nuclei susceptibility. Cavitation Susceptibility Meters (CSM's) are intended to overcome this limitation by directly measuring the active nuclei concentration as a function of the applied tension in a flow through a small venturi tube, where cavitation is induced under carefully controlled conditions. In the original design by Oldenziel (Oldenziel, 1982a; Oldenziel 1982b) a glass venturi is used and cavitation is detected optically. Later applications employ stainless steel venturi tubes, where cavitation bubbles are detected acoustically (Lecoffre and Bonnin, 1979; Le Goff and Lecoffre, 1983; Shen et al., 1984). Among the advantages of CSM's over alternative techniques are the absence of resolution limitations in the minimum size of nuclei they can detect and the relative convenience of data analysis. On the other hand, CSM's are subject to a number of unwanted phenomena, like flow separation, nuclei interference, choking and surface nuclei effects, which severely limit their performance. This paper is part of a systematic investigation of CSM's and critically describes the implementation and operation of the CSM recently developed at the California Institute of Technology (d'Agostino and Acosta, 1983; d'Agostino, 1987; d'Agostino et al., 1989). The principles of operation and the main considerations leading to the current design have been reported in a companion publication (d'Agostino and Acosta, 1991).

## 2 Experimental Apparatus

The design of the CSM described herein is based on the indications of a detailed operational analysis previously re-

[1]Now at the Dipartimento di Ingegneria Aerospaziale, Università di Pisa, 56126, Pisa, Italy.

Contributed by the Fluids Engineering Division for publication in the JOURNAL OF FLUIDS ENGINEERING. Manuscript received by the Fluids Engineering Division July 20, 1989.

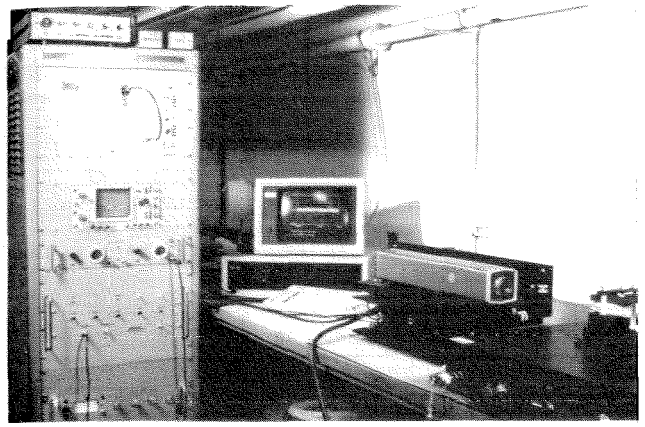

Fig. 1 General view of the CSM experimental apparatus. In the foreground on the right: the I-beams supporting the laser and the baseplate where most of the optical and fluidic components are mounted. In the background: the electronic instrumentation rack (left) and the data acquisition computer (center).

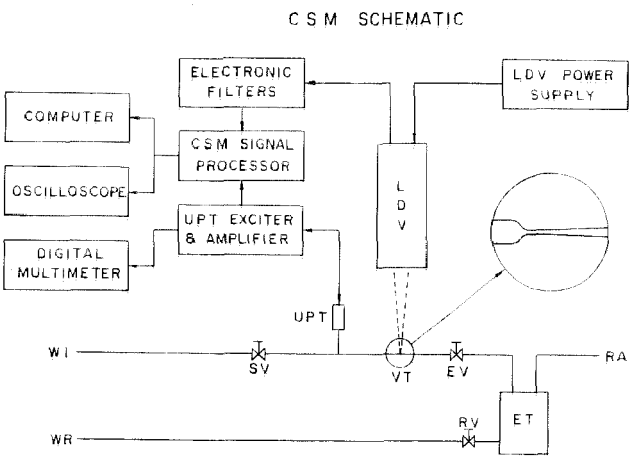


Fig. 2 Schematic of the various components of the CSM experimental apparatus: water inlet (WI), sampling valve (SV), upstream pressure transducer (UPT), venturi tube (VT), exhaust valve (EV), exhaust tank (ET), regulated air pressure line (RA), return valve (RV), water return (WR), laser Doppler velocimeter (LDV).

ported in earlier works (d'Agostino and Acosta, 1983; d'Agostino, 1987) and more recently summarized in a companion paper (d'Agostino and Acosta, 1991). The results of this analysis suggested to develop a CSM where cavitation occurs in the restricted section of a transparent venturi tube. The throat velocity is measured by a back-scattering Laser Doppler Velocity (LDV) and the upstream pressure by an absolute pressure transducer. The LDV signal is also used to detect the occurrence of cavitation at the throat of the venturi tube. The pressure gradient in the venturi throat is ideally zero and thus the slip velocity between the bubbles and the liquid is also zero. Cavitating bubbles are, therefore, accurate velocity indicators. The throat pressure is controlled by adjusting the exhaust pressure and is calculated from the throat velocity and the upstream pressure using Bernoulli's equation for ideal, incompressible, steady, fully-wetted flow, without corrections for viscous effects because the flow possesses a laminar potential core in all operational conditions. The dependence of the active nuclei concentration on throat pressure is measured by repeating the procedure at different exhaust pressures.

A general view of the experimental apparatus is shown in Fig. 1. The electronic instrumentation rack is on the left, the data acquisition and reduction computer is in the center and the optical and fluidic components of the CSM are in the foreground on the right. The connections of the various parts comprising the CSM are illustrated in Fig. 2. The water from the water inlet (WI) passes through the sampling valve (SV), the venturi tube (VT), the exhaust valve (EV) and is finally collected in the exhaust tank (ET). The pressure in the exhaust tank is kept constant by the regulated air pressure line (RA), which is used to control the flow rate and therefore the pressure generated at the throat of the venturi. The static pressure of the sampled water is measured by a pressure transducer (UPT) located upstream of the test venturi. Periodically the sampled water is removed from the exhaust tank through the return valve (RV) and the water return line (WR) by increasing the regulated air pressure. During test runs the dual beam back-scattering Laser Doppler Velocimeter (LDV) monitors the occurrence of cavitation and the flow velocity at the throat of the transparent venturi (VT). The analysis of the signals from the LDV and the upstream pressure transducer is carried out by an especially designed electronic Signal Processor for real time generation and temporary storage of the relevant data. The LDV generates a burst when an inhomogeneity such as a cavity or a suspended particle scatters light during its motion through the focal point. After band-pass filtering this burst ideally consists of a Doppler carrier frequency modulated by a Gaussian-shaped envelope. The Doppler frequency is proportional to the velocity of the scatterer. The amplitude of the burst's envelope is instead mostly related to the scatterer size, although it also depends in a complex way on its shape, optical

## Nomenclature

$A$ = cross-sectional area
$C_c$ = venturi contraction coefficient
$C_e$ = venturi expansion coefficient
$D$ = venturi diameter
$f$ = probability density distribution
$L$ = length
$M$ = number of data groups
$n(p_t)$ = concentration of nuclei with critical pressure not smaller than $p_t$
$N$ = integer number
$N_b$ = number of cavitation events or bubbles
$N_{zc}$ = number of zero crossings
$p$ = pressure
$p_t$ = venturi throat pressure
$p_u$ = venturi upstream pressure
$q$ = volume flux
$R$ = venturi radius
$t$ = time
$t_s$ = sampling time
$T$ = temperature
$T_b$ = arrival time of a cavitation event or bubble
$T_g$ = Doppler gate time
$T_p$ = arrival time of a velocity tracer or particle
$u$ = velocity
$u_t$ = venturi throat velocity
$\alpha$ = air content
$\delta$ = boundary layer thickness
$\epsilon$ = error
$\bar{\nu}_b$ = average cavitation event rate
$\sigma$ = standard deviation
$\sigma^2$ = variance

### Subscripts

$b$ = bubble or cavitation event
$c$ = venturi tub contraction
$e$ = venturi tube exhaust
$o$ = reference conditions
$p$ = particle or velocity tracer
$s$ = sample
$t$ = venturi tube throat
$u$ = upstream
$zc$ = zero crossing

### Acronyms

CSM = Cavitation Susceptibility Meter
LDV = Laser Doppler Velocimeter

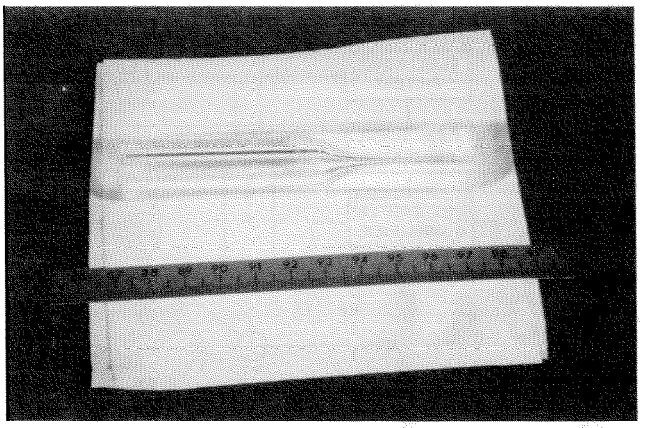

**Fig. 3 Close-up view of the CSM venturi tube No. 1. A cylindrical shell of cast transparent resin contains the glass blown venturi tube for mechanical protection and easy installation. The contraction ratio of the tube is about 1/100, the throat diameter is about 1 mm and the exit diameter is about 1.2 mm.**

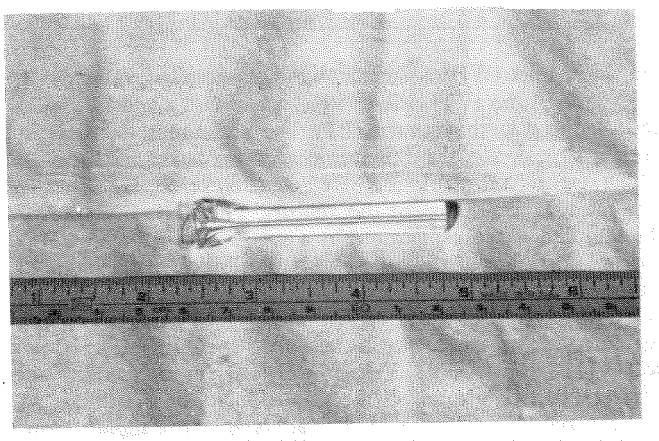

**Fig. 4 Close-up view of the CSM venturi tube No. 2. This blown glass venturi has thicker walls, a contraction ratio of about 1/100, a throat diameter of about 1 mm, a long straight section after the diffuser and an exhaust diameter of about 1.2 mm.**

properties and on the location of its trajectory through the LDV focal point. The CSM Signal Processor uses the intensity and the Doppler modulated frequency of the LDV bursts to respectively monitor the occurrence of cavitation and to measure the flow velocity. The instantaneous upstream pressure of the water is provided by the output of the pressure transducer. At the conclusion of each run the data are transferred to the minicomputer for final acquisition, storage and reduction. The LDV signal is normally monitored by an oscilloscope and the signal of the upstream pressure transducer by a digital multimeter.

Two types of glass venturi tubes have actually been used. The first type, indicated as tube No. 1, is an extremely fragile blown glass venturi contained in a cylindrical shell of transparent acrylic resin (see Fig. 3) for mechanical protection and connection to the hydraulic lines. The second type of glass venturi, indicated as tube No. 2, has much thicker walls and can therefore be directly connected to the hydraulic lines without mechanical protection. It is shown in detail in Fig. 4. These two venturi tubes have very similar fluid mechanical characteristics. They both have about the same throat diameter ($D_t \simeq 1$ mm), the same throat section length ($L_t \simeq 5$ mm) and the same geometrical contraction and expansion ratios ($C_c \simeq 1/100$ and $C_e \simeq 1.44$, respectively). Hence, the velocity profile determined from fully wetted flow measurements with artificial seeding using the LDV is also very similar in the two venturis and the corresponding minimum pressure developed is in both cases $p_{t_{min}} \simeq -35$ kPa. The most important fluid mechanical

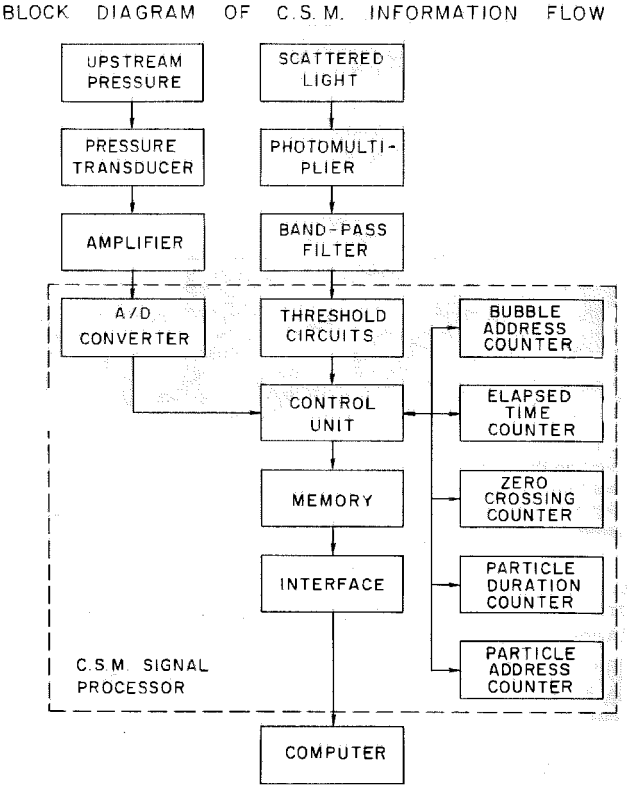


**Fig. 5 Block diagram of the information flow in the CSM Signal Processor**

difference between the two venturi tubes is the different length of the exit section, much shorter in the venturi No. 1 (only a few mm) than in the venturi No. 2 (about 3 cm). As a consequence, the flow in the second venturi is considerably more stable with respect to the insurgence of cavitation-separation.

## 3 Data Acquisition and Reduction

A simplified block diagram of the CSM signal processing and data acquisition is shown in Fig. 5. The output of the photomultiplier is band-pass filtered for separating the Doppler frequency from the electronic noise and sent to the CSM Signal Processor, where it is amplified before entering the threshold circuits. Here a zero level and two couples of adjustable, symmetric threshold levels are used to reject the residual noise and to discriminate valid Doppler bursts coming from a velocity tracer from the ones coming from a cavitation event. For simplicity cavitation events will be indicated as bubbles and velocity tracers as particles, although in practice smaller cavities probably represent the majority of the velocity tracers recognized by the CSM Signal Processor during a typical CSM run. The information from the threshold circuits is used by the Signal Processor to control five counters and to generate, collect and temporarily store in real time the following data:

- when a cavitation event (bubble) is recognized:
  1. the occurrence time measured from the beginning of the run (bubble elapsed time, $T_b$);
- when a velocity tracer (particle) is recognized:
  1. the occurrence time measured from the beginning of the run (particle elapsed time, $T_p$);
  2. the duration of the Doppler burst (particle gate time, $T_g$);
  3. the number of zero crossings of the Doppler burst $N_{zc}$;
  4. the upstream water pressure $p_u$;

A maximum of 1024 cavitation bubbles and velocity tracers can be independently recorded at a maximum acquisition rate

of about 10000 events per second. At the conclusion of each run the data collected by the CSM Signal Processor are serially transferred to the microcomputer for final acquisition, storage on a magnetic disk and reduction.

The data reduction develops through the following steps:

1 zero crossing validation and statistical filtering of the Doppler frequency and upstream pressure data;
2 computation of the average potential core velocity, of the potential core velocity data standard deviation and of the boundary layer thickness;
3 computation of the average throat pressure and of the throat pressure data standard deviation;
4 validation of the arrival times of cavitation events and velocity tracers;
5 computation of the observed and expected occurrence frequency distributions of the delay times between cavitation events;
6 computation of the unstable nuclei concentration and of its standard deviation.

During the first step Doppler frequency data are computed by dividing the number of zero crossings of each burst by twice its duration. To reject spurious bursts, only counts with a preselected minimum number of zero crossings are used (zero crossing validation). Both the Doppler frequency data and the upstream pressure data contain a relatively small number of outliers due to various noise sources in the electronics. In addition, the Doppler frequency data may sometimes contain a significant number of low frequency readings from scatterers deep inside the venturi boundary layers. To eliminate the noise and to isolate the velocity information primarily coming from the venturi's potential core the Doppler frequency data are statistically filtered by only retaining those readings whose deviation from their average values does not exceed a preset multiple of their standard deviation (usually three standard deviations). The same procedure is also applied to the upstream pressure data, leading to the determination of the average upstream pressure $\bar{p}_u$ and of the upstream pressure data standard deviation $\sigma_{p_u}$.

The computation of the average potential core velocity, of the potential core velocity data standard deviation and of the boundary layer thickness (step 2) is carried out as follows. First the observed occurrence frequency distribution of the measured velocity data is calculated in the form of a histogram chart. When boundary layer effects are important and their role is not masked by other factors, this distribution is negatively skewed and therefore its third central moment is negative. If this is not the case the expected value and the standard deviation of the observed distribution are simply used to compute the average potential core velocity $\bar{u}_t$ and the standard deviation of the potential core velocity data $\sigma_{u_t}$, while the boundary layer thickness $\delta$ is taken to be zero. Otherwise, assuming uniformly distributed scatterers throughout the venturi cross-section, a theoretical probability distribution of the measured velocity is derived that parametrically depends on $\bar{u}_t$, $\sigma_{u_t}$ and the ratio of the boundary layer thickness to the local duct radius $\delta/R_t$. These parameters are then determined by fitting the theoretical distribution to the observed one. This process results in a slightly higher estimate of the average throat velocity and in a small reduction of the standard deviation of the throat velocity data depending on the value of the parameter $\delta/R_t$.

The venturi throat pressure $p_t$ (step 3) is deduced from the measurements of the upstream pressure $p_u$ and of the throat velocity $u_t$ using Bernoulli's equation for ideal, incompressible, steady, fully wetted flow. An unavoidable problem associated with this technique is that the throat pressure, being inherently small compared to the upstream pressure and the kinetic pressure drop, is expressed as the difference of two almost equal quantities. Thus, small relative errors in the evaluation of these quantities lead to a much larger relative error for the throat pressure. The statistical analysis for the determination of the average value $\bar{p}_t$ and the standard deviation $\sigma_{p_t}$ of the throat pressure data $p_t$ is carried out assuming that the two independent data populations $p_u$ and $u_t$ are normally distributed about their average values $\bar{p}_u$ and $\bar{u}_t$, with variances $\sigma^2_{p_u}$ and $\sigma^2_{u_t}$, respectively.

Clearly, the arrival times of LDV bursts are monotonically increasing and, in steady conditions, approximately proportional to their index. These properties are used to validate the data and to assess the uniformity of both the sample and the test conditions. First, the linear regression curve of the arrival times as a function of their index is calculated. Then, the data which are not in monotonically increasing order and whose deviation from the regression line is the largest are eliminated, in order to eliminate spurious readings (step 4).

The observed frequency distribution of the time $t$ between successive cavitation events is calculated and a histogram chart is constructed by sorting the $N_b$ data in, say, $M$ groups equally spaced in time for comparison with the expected Poissonian exponential distribution $f(t) = N_b\bar{\nu}_b e^{-\bar{\nu}_b t}$, where $\bar{\nu}_b = N_b/t_s$ is the average arrival rate of cavitation events during the sampling time $t_s$ (step 5). Finally, the volume flow rate $q = A_t\bar{u}_t$ is used to estimate the unstable nuclei concentration $n(p_t) = N_b/t_s q$ and its standard deviation $\sigma_n = \sqrt{N_b}/t_s q$ (step 6).

## 4 Experimental Procedure, Results, and Discussion

The calibration of the CSM system has been carried out using a mercury barometer for the upstream absolute pressure transducer and a rotating disk in air as a source of a finely controlled velocity field for the LDV. The overall accuracy (linearity plus repeatability) of the calibrations was better than 200 Pa for the upstream pressure transducer over the range 20 to 160 kPa, and 0.05 m/s for the LDV over the range 9 to 22 m/s. Thus, in general, the CSM instrumentation error was always negligible with respect to the inherent dispersion of the measured quantities.

The experimental procedure for measuring the water quality with the CSM is relatively simple. The water source is connected to the CSM test section with the shortest possible tubing, taking care to avoid abrupt changes of the duct internal section. An overflow line is also used to reduce as much as possible the transfer time of the sample to the CSM. The temperature of the sampled water is measured with a thermometer and its air content with a manometric van Slyke meter before each CSM run.

The location of the LDV focal point is very important for obtaining high quality repeatable results from the CSM. Experience showed that the best location is at the end of the venturi throat section. This choice provides better LDV signal strength, due to the larger size of the scattering bubbles, with acceptable dispersion of the velocity data. The electronic settings also are of crucial importance for the operation of the CSM, since they determine the number of LDV bursts recognized and counted as cavitation events. Proper choice of these settings depends on the correlation of the scatterer size to its LDV signature and on the definition of a general criterion for discriminating in dynamic conditions unstable cavitating nuclei from stable ones. This first aspect can be partially addressed by calibrating the LDV signal from cavities of known sizes, for example by monitoring the sampled water with holographic methods (d'Agostino et al., 1989; d'Agostino and Green, 1989). The discrimination of unstable cavitating nuclei, however, is essentially equivalent to the definition of the cavitation inception conditions, which is still an open problem in cavitation research. Until these two problems are satisfactorily solved, the selection of the electronic settings of the CSM remains, at least to some extent, arbitrary. In the present case the electronic settings were chosen trying to optimize the re-

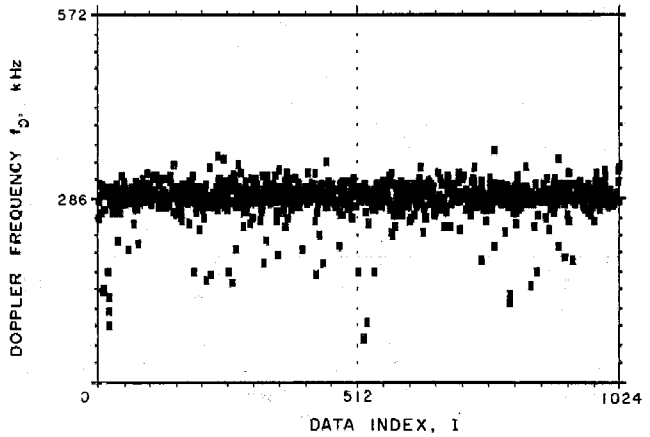


**Fig. 6 Doppler frequency data $f_D$ as a function of the data index $I$ in a typical CSM run. The data refer to a tap water sample with initial pressure $p_o$ = 1 atm, temperature $T$ = 21°C, air content $\alpha$ = 20.5 ppm, throat pressure $p_t$ = −15 kPa and velocity $u_t$ = 14.8 m/s.**

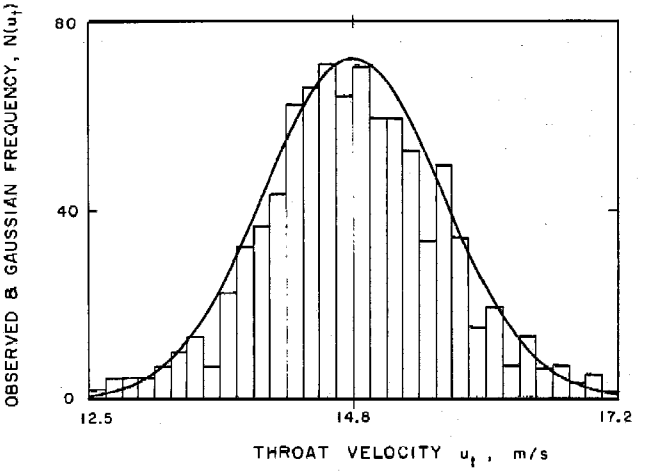


**Fig. 7 Observed distribution of filtered throat velocity data (histograms) compared to the Gaussian distribution (solid line) of equal mean and standard deviation for the data sample of Fig. 6**

sponse of the electronics and to ensure the applicability of the same settings to the whole range of the expected operational conditions.

The results reported in this section have been obtained testing tap water in the venturi tubes No. 1 and No. 2 briefly described in the previous section. Three different flow regimes have been observed:

- traveling bubble cavitation;
- cavitation-separation and sheet cavitation;
- spot and resonant cavitation.

Clearly only the first one is the nominal operational regime of the CSM where meaningful water quality measurements can be made. The others involve unwanted phenomena, which often perturb the flow conditions in an uncontrollable way and prevent the possibility of reliably measuring the active cavitation nuclei concentration in the sampled water. Therefore, for conciseness, they will not be examined here.

The traveling bubble flow regime is characterized by the random occurrence of cavitation bubbles in the CSM venturi and has been observed in both venturi tubes No. 1 and No. 2. The bubbles start to develop in the bulk of the liquid in the upstream region of the venturi's throat section, travel downstream reaching their maximum size somewhere in the diffuser or sometimes in the exit section, and later collapse. Under stroboscopic light the bubbles appear approximately spherical, at least during their growth phase. The length of the region where cavitation bubbles can be observed, their maximum size and occurrence rate depend on the flow conditions, clearly increasing with the throat tension and the velocity of the flow. In the venturi tube No. 2 (the only one where the entire life cycle of the cavitation bubbles can be observed) the length of the cavitation region ranges from about 5 to 25 mm. The maximum size of the bubbles varies greatly and can even be comparable to the local diameter of the venturi. Optical observation also indicates that larger bubbles occur when the cavitation event rate is relatively low. This behavior suggests the possible presence of significant interactive effects among the bubbles at high concentrations and is directly related to the general problem of flow saturation, which will be discussed later.

Some of the physical raw data and of the reduced data from a typical CSM run of a tap water sample with an air content of 20.5 ppm at 21°C are shown in Fig. 6 through Fig. 8. The water sample, initially at atmospheric pressure, was tested in the venturi tube No. 2 at a throat pressure of −15 kPa corresponding to a velocity of 14.8 m/s.

The Doppler frequency data in the first plot of Fig. 6 are centered about their average value indicated on the scale. The

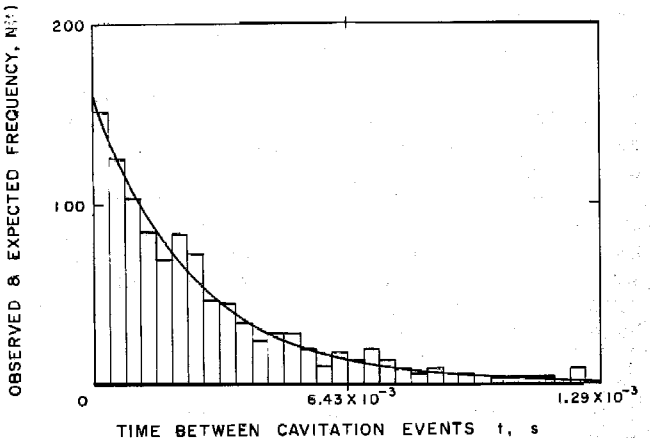


**Fig. 8 Observed distribution of time intervals between cavitation events (histograms) in a typical CSM run compared to the theoretical exponential distribution (solid line) of equal average arrival rate. The data refer to the tap water sample of Fig. 6**

dispersion of the data is mainly due to the intrinsic slightly unsteady nature of the flow and to the non-uniformity of the velocity profile in the venturi. However, this data set also contains a small but significant number of low frequency readings. Some of these readings do not appear to be randomly distributed during the run, but rather seem to occur sequentially in small groups. Experience with the operation of the CSM indicates that they are probably coming from cavities rather than, for example, from small particles normally present in the boundary layer. Most likely they are due to bubbles originating from the disintegration of small attached cavities from surface nuclei under the action of the incoming flow and later swept downstream through the LDV probe volume before they had time to accelerate to the surrounding flow velocity. This conclusion is also supported by the observation that cavitation events occasionally occur in clusters, which correspond to short, almost horizontal stretches in the plot of the bubble arrival time data.

In the second plot (Fig. 7) the histogram chart representing the velocity data distribution is compared to the Gaussian curve of equal average value and standard deviation. Readings deviating from the mean more than three standard deviations have been eliminated. Note that the observed distribution of velocity data seems to follow rather closely a normal distribution and does not display any appreciable skewness which could be attributed for example to the effects of the boundary layers, as previously mentioned. Experience from other runs

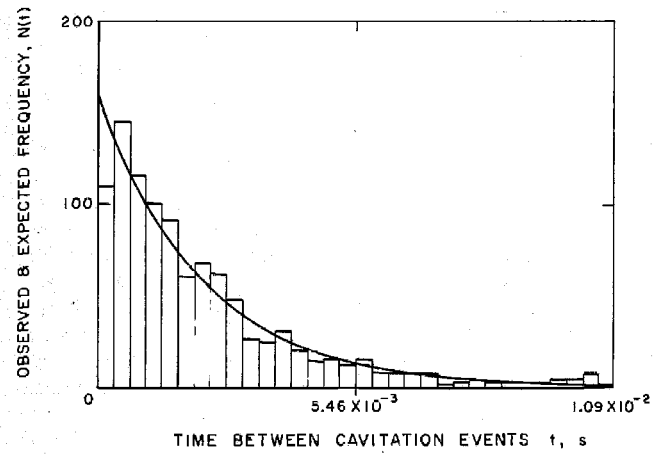


**Fig. 9 Observed distribution of time intervals between cavitation events (histograms) slightly deviating from the theoretical exponential distribution (solid line) as a consequence of short range bubble interference effects**

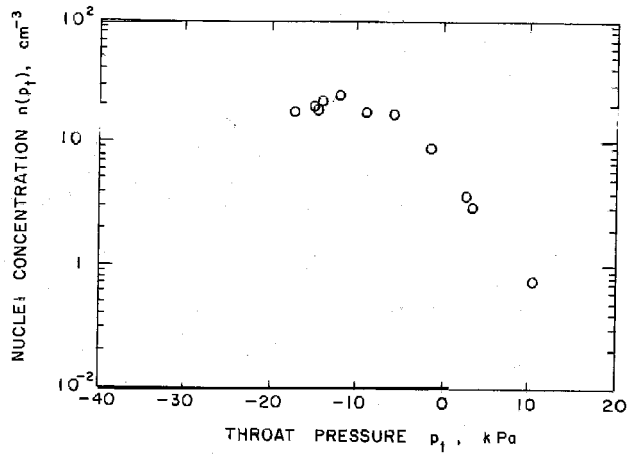


**Fig. 10 Cavitating nuclei concentration $n(p_t)$ measured by the CSM as a function of the venturi throat pressure $p_t$ in a sample of tap water with temperature $T$ = 21°C and air content $\alpha$ = 20.5 ppm**

showed that the skewness of velocity distributions is usually small in both directions and probably statistically insignificant, as if the biasing effects of the boundary layer were unimportant or masked by some other phenomenon. Therefore the estimates of the ratio of the boundary layer thickness computed from the observed negative skewness of the velocity data distribution should be regarded with some skepticism, despite the fact that they never gave unrealistic results.

In the last plot (Fig. 8) the histogram chart representing the distribution of the observed time intervals between cavitation events is compared to the Poissonian exponential distribution expected to describe the occurrence of cavitation when the flow conditions are constant and the cavitation events are uncorrelated. This comparison provides a way to assess the importance of short range nuclei interference effects at the throat of the CSM venturi due to the inhibiting action that the pressure perturbations from a growing cavity can exert on the growth of neighboring nuclei. Clearly, this kind of interaction especially penalizes the occurrence of the shortest time intervals between successive cavitation events with respect to the theoretical Poissonian distribution. The data from Fig. 8 do not show any evidence of important short range bubble interference. For comparison, an example of a distribution deviating from the expected exponential behavior as a consequence of nuclei interference effects is shown in Fig. 9 for a different CSM run. In general these effects in CSM flows are not large. At most they affect a few percent of the total number of cavities and only tend to appear at heavier cavitation rates, when the separation between cavitating nuclei is proportionally reduced. This is not surprising when considering that the minimum average separation of cavitation bubbles is comparable to the length of the CSM venturi tube even at the highest cavitation rates. Clearly, more cavities are actually present in the flow whose LDV signatures are not large enough for them to be recognized as cavitation events by the CSM Signal Processor. For these cavities short range interference effects are likely to be more significant.

When a large number of cavities is continuously present in the cavitation region of the CSM venturi the collective effects of the bubble volume changes produce a global, permanent increase of the pressure throughout the venturi test section (choked flow conditions). In this situation the tube is saturated and the maximum tension that venturi tube can develop at any given flow rate is reduced, as it will be shown later in this section. However, the pressure experienced by any one bubble is not appreciably modified by the presence of the neighboring ones, since saturation is a large scale effect due to the collective contribution of many cavities widely distributed in the flow.

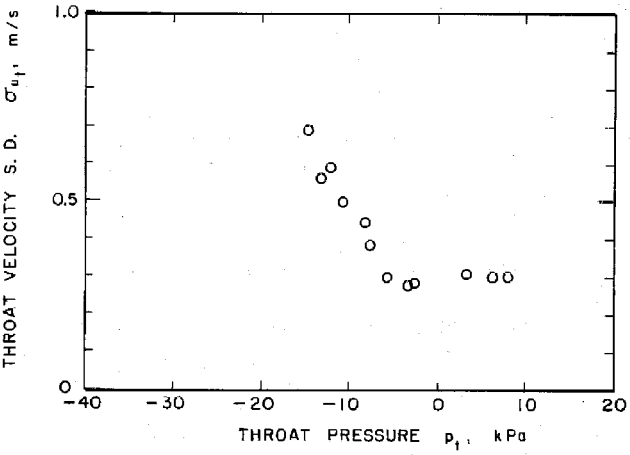


**Fig. 11 Standard deviation of the throat velocity data $\sigma_{u_t}$ as a function of the throat pressure $p_t$ in the tap water sample of Fig. 10**

Therefore this kind of bubble interference will affect the average cavitation rate but will not be reflected in an anomalous distortion of the observed distribution of the time intervals between cavitation events. Clearly, saturation phenomena tend to increase with the concentration of unstable cavitation nuclei in the water sample and with the tension they are exposed to and impose limitations to the range of liquid quality measurements which can be carried out with the CSM.

An example of the application of the CSM to the measurement of the cavitation nuclei concentration as a function of the venturi throat pressure by means of repeated runs on a sample of tap water at 21°C with a dissolved air content of 20.8 ppm is shown in Fig. 10 and Fig. 11. These results are generally representative of CSM water quality measurements on other tap water samples in similar conditions. At first the concentration of cavitation nuclei increases about exponentially with the applied tension, as also reported by other investigators (Oldenziel, 1982a; Shen and Gowing, 1985; Shen et al., 1986). When the throat pressure is further reduced below about −7 kPa the concentration of cavitation nuclei reaches a maximum ranging from 20 to 40 $cm^{-3}$ and remains nearly constant thereafter. The observed behavior of the concentration of cavitation nuclei probably reflects the actual lack of cavitation nuclei which become active when the throat pressure is lowered below about −7 kPa. In this case a further decrease of the throat pressure would simply produce a more violent growth and collapse of the available population of active nuclei. Larger perturbations would then be induced in the flow,

thus generating the parallel increase of the velocity data standard deviation from a previously constant value that is clearly apparent in Fig. 11. This interpretation has also been favorably tested by comparison of CSM results with holographically determined nuclei concentration density distributions (d'Agostino et al., 1989; d'Agostino and Green, 1989). Finally, note that, assuming in first approximation that the throat pressure is correctly measured also in the presence of heavy cavitation, the minimum pressure generated by the CSM venturi in the run of Fig. 10 is of the order of $-15$ kPa and therefore considerably higher than the venturi can develop in the absence of extensive cavitation. It appears that saturation phenomena are responsible for the observed decrease of the maximum achievable tension in the venturi and the consequent performance limitations.

At given settings of the CSM the accuracy in the determination of the water quality is due to the errors in the measurement of the cavitating nuclei concentration and of the average throat pressure. With good approximation the throat pressure data are normally distributed and the occurrence of cavitating nuclei is a Poisson process, provided that the flow conditions are constant during the run. Then, both the above errors are inversely proportional to the square root of the size of the data sample (Browlee, 1960) and therefore can be significantly reduced by averaging the measured quantities on a sufficiently large number of data. Since the number of filtered data is usually close to 900, the relative r.m.s. error of the measurement of the cavitating nuclei concentration is rather small, of the order of a few percent. The standard deviation of the throat pressure data is quite large in relative sense due to the inherent dispersion of the throat velocity data and to the small value of the pressure at the CSM venturi throat. Values of about 5 to 10 kPa for the standard deviation of the throat pressure data are representative of the results usually obtained from CSM runs. As mentioned earlier, this value must be divided by the square root of the sample size in order to obtain the standard deviation of the average throat pressure. With the same size of data sample as previously assumed the corresponding error in the determination of the average throat pressure is therefore of the order of a few hundred Pascals. The above expected errors are both relatively small, but it should be born in mind that they strictly refer to the measurement process alone. In a broader sense the indetermination in the measurement of the water quality also includes the effects of the uncertainties in the relationship between the LDV signal intensity and the size of cavitating bubbles and in the discrimination of unstable nuclei from the stable ones. The former of these effects is related to the specific nuclei detection technique used in the CSM and could presumably be resolved to some extent by calibrating the instrument response with cavities of known sizes, as previously suggested. The latter is instead shared by all currently devised techniques of cavitation nuclei detection. The inclusion of all error sources involved makes the measurement of the liquid quality with CSM's (and with other alternative methods) considerably more uncertain than it would first appear from the above considerations.

## 5 Conclusions

The following conclusions can be drawn from the available experience on the CSM system at the present stage of the project:

- three different flow regimes have been observed in the CSM venturi tube:
  1 travelling bubble cavitation (during normal operation);
  2 cavitation-separation and sheet cavitation;
  3 spot and resonant cavitation.
- the proposed design concept has been successfully demonstrated in all its components;
- the CSM is able to measure the concentration of active cavitation nuclei as a function of the throat pressure over an extended range of applied tensions;
- the maximum value of the tension currently attainable ($-35$ kPa) is often insufficient for cavitating waters with relatively low nuclei content;
- at high nuclei concentrations flow saturation produces a generalized increase of the pressure and a parallel decrease of the velocity throughout the venturi throat section and therefore limits the performance of the CSM by reducing the maximum value of the tension exerted on the liquid;
- contrary to preliminary expectations, the arrival of cavitation events remains nearly Poissonian also at high cavitation results. Therefore saturation does not produce important short range interference effects between cavitating nuclei nor, consequently, poses significant limitations to the measurement of the concentration of active cavitation nuclei other than those due to the reduction of the maximum tension applied to the liquid;
- the maximum measurable concentration of active cavitation nuclei in the water samples tested so far appears to be limited by the available supply of nuclei in the samples rather than by the occurrence of saturation;
- active cavitation nuclei concentrations up to about 40 $cm^{-3}$ have been recorded with little evidence of short range interference effects between cavitating bubbles;
- the flow is very sensitive to laminar separation in the diffuser, which limits the minimum throat pressure currently attainable to about $-35$ kPa;
- cavitation-separation and sheet cavitation frequently interfere with the normal operation of the CSM;
- the possibility of measuring the velocity of individual cavities at the venturi throat represents a powerful and unique mean for discriminating the cavities produced by free-stream nuclei from the ones originated from surface nuclei and for introducing corrections to the CSM measurements when necessary;
- the possibility of recording the transit time of cavitating bubbles is extremely useful to assess the importance of short range interference effects from the statistical properties of the cavitation process;
- the measurements of the cavitation nuclei number concentration density distributions in tap water samples obtained using the CSM show little dispersion and good repeatability;
- comparison of the CSM with a reliable nuclei detection method (holography) is indispensable in order to "properly" choose the electronic thresholds for the discrimination of cavitation events and in order to correctly interpret some of the observed results.

## Acknowledgments

This research has been funded by the Office of Naval Research and by the Naval Sea Systems Command General Hydromechanics Research Program administered by the David W. Taylor Naval Ship Research and Development Center. The North Atlantic Treaty Organization-Consiglio Nazionale delle Ricerche, Italy, has also contributed to the support of this work through a 1982 and a 1983 Fellowship for Technological Research. Special thanks to Dr. T. T. Huang of DTNSRDC for his interest in this work, to Mr. Joe Fontana, Mr. Elton Daly, Mr. Rich Eastvedt, Mr. Leonard Montenegro, Mr. John Lee and to Miss Cecilia Lin of the Caltech staff for their assistance in the completion of the experiment and to Dr. Haskel Shapiro, Mr. Bob Kirkpatrick and their group for the design and implementation of the custom-made electronics.

## References

Billet, M., 1986, "The Importance and Measurement of Cavitation Nuclei," *Advancements in Aerodynamics, Fluid Mechanics and Hydraulics*, Minneapolis Minn., pp. 967-989.

Billet, M., 1985, "Cavitation Nuclei Measurement—A Review," *ASME Cavitation and Multiphase Flow Forum*, Albuquerque, N.M., pp. 31–38.

Browlee, K. A., 1960, *Statistical Theory and Methodology in Science and Engineering*, Wiley.

Chahine, G. L., and Shen, Y. T., 1986, "Bubble Dynamics and Cavitation Inception in Cavitation Susceptibility Meters," ASME JOURNAL OF FLUIDS ENGINEERING, Vol. 108, pp. 444–452.

d'Agostino, L., 1987, "Experimental and Theoretical Study on Cavitation Inception and Bubbly Flow Dynamics," Ph.D. thesis, Report No. Eng. 183.16, California Institute of Technology, Pasadena, Calif.

d'Agostino, L., and Acosta, A. J., 1983, "On the Design of Cavitation Susceptibility Meters," *American Towing Tank Conference*, Hoboken, N.J.

d'Agostino, L., and Acosta, A. J., 1991, "A Cavitation Susceptibility Meter With Optical Cavitation Monitoring—Part One: Design Concepts," published in this issue pp. 261–269

d'Agostino, L., Thai Pham and Green, S., 1989, "Comparison of a Cavitation Susceptibility Meter and Holographic Observation for Nuclei Detection in Liquids," ASME JOURNAL OF FLUIDS ENGINEERING, Vol. 111, No. 2, pp. 197–203.

d'Agostino, L., and Green, S. I., 1989, "Simultaneous Cavitation Susceptibility Meter and Holographic Measurements of Nuclei in Liquids," *ASME Cavitation and Multiphase Flow Forum*, San Diego, California, USA.

Godefroy, H. W. H. E., Jansen, R. H. J., Keller, A. P., and van Renesse, R. L., 1981, "Comparison of Measuring and Control Methods of the Water Quality with Respect to Cavitation Behavior," Delft Hydraulics Laboratory Publication.

Ito, Y., and Oba, R., 1980, "Cavitation Observations through a Fine Laser Beam Technique," Report No. 337, Institute of High Speed Mechanics, Tohoku University.

Knapp, R. T., Daily, J. W., and Hammitt, F. G., 1970, *Cavitation*, McGraw Hill, N.Y.

Lecoffre, Y., and Bonnin, J., 1979, "Cavitation Tests and Nucleation Control," *International Symposium on Cavitation Inception*, New York, N.Y., pp. 141–145.

Le Goff, J. P., and Lecoffre, Y., 1983, "Nuclei and Cavitation," *14th Symposium on Naval Hydrodynamics*, National Academy Press, pp. 215–242.

Oldenziel, D. M., 1982a, "A New Instrument in Cavitation Research: the Cavitation Susceptibility Meter," ASME JOURNAL OF FLUIDS ENGINEERING, Vol. 104, pp. 136–142.

Oldenziel, D. M., 1982b, "Utility of Available Instruments during Cavitation Tests," *Proceedings of Symposium on Operating Problems of Pump Stations and Power Plants*, IAHR, Amsterdam.

Oldenziel, D. M., 1979, "New Instruments in Cavitation Research," *International Symposium on Cavitation Inception*, New York, N.Y., pp. 111–124.

Oldenziel, D. M., Jansen, R. H. J., Keller, A. P., Lecoffre, Y., and van Renesse, R. L., 1982, "Comparison of Instruments for Detection of Particles and Bubbles in Water during Cavitation Studies," *Proceedings of Symposium on Operating Problems of Pump Stations and Power Plants*, IAHR, Amsterdam.

Shen, Y. T., Gowing, S., and Pierce, R., 1984, "Cavitation Susceptibility Meters by a Venturi," *International Symposium on Cavitation Inception*, ASME Winter Annual Meeting, pp. 9/18.

Shen, Y. T., and Gowing, S., 1985, "Scale Effects on Bubble Growth and Cavitation Inception in Cavitation Susceptibility Meters," *ASME Cavitation and Multiphase Flow Forum*, Albuquerque, New Mexico, pp. 14–16.

Shen, Y. T., Gowing, S., and Eckstein, B., 1986, "Cavitation Susceptibility Measurements of Ocean Lake and Laboratory Waters," David W. Taylor Naval Ship Research and Development Center, Report DTNSRDC-86/D19.

## 11ADMC – Hobart, Australia, 14–18, December, 1992

The Eleventh Australasian Fluid Mechanics Conference will be held at the University of Tasmania from Monday 14, December, 1992 until Friday 18, December 1992. Papers on all aspects of fundamental and experimental fluid mechanics may be presented and published in the proceedings. Conferences in this series are held once every three years only. Invited keynote papers will review aspects of mixing, combustion, computational methods, hydraulics, turbomachines, hydrodynamics and occanography. Abstracts for preliminary review should be submitted to the Conference Secretariat by 31, January, 1992. These and other enquiries concerning the conference should be directed to: 11AFMC Secretariat, Department of Civil & Mechanical Engineering, University of Tasmania, GPO Box 252C, Hobart, 7001, Australia. (Fax 002-234611).